Journal of Energy Storage 22 (2019) 36–43

Contents lists available at ScienceDirect

Journal of Energy Storage

journal homepage: www.elsevier.com/locate/est

The design and impact of *in-situ* and operando thermal sensing for smart energy storage

Joe Fleming[a], Tazdin Amietszajew[a,*], Jerome Charmet[a], Alexander John Roberts[a], David Greenwood[a], Rohit Bhagat[b]

[a] WMG, University of Warwick, Coventry, UK
[b] Coventry University, Coventry, UK

ARTICLE INFO

Keywords:
Li-ion
Thermal management
In-situ
Cell instrumentation
Sensors
Smart cells
Distributed monitoring
Power mapping, 18650 cells
Pouch cells
Battery management
Cell performance
Safety limits

ABSTRACT

Lithium-ion is increasingly the technology of choice for battery-powered systems. Current cell performance monitoring, which relies on measurements of full cell voltage and sporadic surface temperature, does not provide a reliable information on the true internal battery state. Here, we address this issue by transforming off the shelf cells into smart systems by embedding flexible distributed sensors for long-term *in-situ* and operando thermodynamic data collection. Our approach, which enables the monitoring of the true battery state, does not impact its performance. In particular, our results show that this unprecedented methodology can be used to optimise the performance and map the safety limits of lithium-ion cells. We find that the cell core temperature is consistently and significantly higher than the surface temperature, and reveal a breach of safety limits during a rapid discharge test. We also demonstrate an application of a current considerably higher than the manufacturers' specification, enabling a significant decrease in charging time, without compromising the cell's thermal stability. Consequently, this work on cell instrumentation methodology has the potential to facilitate significant advances in battery technology.

1. Introduction

The development of a civilisation is tied to its growing energy consumption [1], and current mobility requirements combined with a drive towards cleaner energy sources has boosted the demand for portable power sources. Over the last decades, a range of technologies were developed, however, due to its significant technological advantages including; large capacity, no self-discharge and a high output voltage [2–6], lithium-ion has emerged as the technology of choice for portable electronics, off-grid storage and electric vehicles. Li-ion cells have revolutionised 21 st century society by enabling mobile communications, portable electronics and implanted medical devices. However, the drive to push the performance of such cells, e.g. through a reduction of the charging time or an increase capacity, is often limited by safety concerns. Indeed, safety issues intrinsic to this technology [7–9] have led to catastrophic failures of portable devices such as mobile phones, electronic cigarettes as well as electric vehicles.

The prevailing approach for preventing unexpected events occurring within battery system is by employing a battery management system (BMS). The purpose of the BMS is to control the flow of energy to and from the battery system, monitor for errors and apply real-time corrective actions if necessary. The typical methodology of characterizing a battery system is by using two factors - the state of charge (SoC) and state of health (SoH). SoH is a particular measure of the performance characteristics such as peak-current delivery, cycle-time and capacity degradation, while the SoC quantifies the present capacity of a cell. To manage, diagnose and predict batteries SoH and SoC, the BMS utilises a small array of sensors, alongside computational algorithms. Typically, such sensors are attached to the surface of a selected number of cells [10] monitoring voltage and temperature. However, thermal management systems, environmental disturbances and unforeseen events within the module can cause sensors to produce false or highly inaccurate data [11]. Consequently, our knowledge of the cells' true internal state in real-life is very limited, resulting in an inability to detect hot-spots formation which can reduce the cell performance or even result in catastrophic failure events [12], rapid aging or thermal expansion. Besides, it was shown that temperature is a major factor affecting cells performance [13–16], leading to SoH degradation, performance issues and safety concerns [17]. Ergo, the strategy of single point surface measurements is not sufficient to provide an accurate SoH

* Corresponding author.
E-mail address: t.amietszajew.1@warwick.ac.uk (T. Amietszajew).

https://doi.org/10.1016/j.est.2019.01.026
Received 9 October 2018; Received in revised form 29 November 2018; Accepted 26 January 2019

indication or reliable cell diagnosis.

Such challenges can be addresses through the development of *in-situ* distributed and operando temperature measurements of cells. Even though some attempts were made in this direction, very limited information is available regarding such approaches, their implementation and their long-term stability. Importantly, the various attempts to develop *in-situ* distributed measurement of temperature [15,16,18], fail to provide information regarding the impact of such measurement upon the electrochemical system.

In particular, *in-situ* approaches using thermocouples have been explored [10,14,19–25], however such systems are limited to measuring relative temperature changes and require a cold junction element and analogue conditioning circuits to compensate for their poor sensitivity. Furthermore, it is not possible to multiplex thermocouples to a single wire, thus limiting their miniaturization, adding further points of failure and increasing the complexity, mass and cost of the system. Further *in-situ* studies [16,18] were performed with optical fibre sensors. However, such sensors are affected by mechanical stress, thus limiting the accessible locations within the cell and the confidence with which the temperature could be observed. Besides, their implementation is complex and require high capital cost. Furthermore, fibre technology is extremely sensitive to bending and vibration causing significant long-term reliability issues, severely limiting real-life application.

In the following paper we show major developments in this respect, enabling unprecedented high-precision distributed in operando monitoring of pouch and cylindrical format cells over a long period of time. This long-term stability was achieved by modifying the discrete thermistor elements to render them immune to the Li-ion cells' harsh environmental conditions before their integration into the smart cells. Our approach, which enables the monitoring of the true battery state, paves the way for a deeper knowledge of battery performance. In particular, we highlight an early safety limit breach in the case of rapid discharge and show that the charging time of certain cells can be significantly reduced without compromising the safety limits.

We also show that our approach has no significant influence on the performance of the cells. We have conducted a series of tests, including time domain oriented cycling ageing, frequency domain related Electrochemical Impedance Spectroscopy, X-Ray *in-situ* inspection and post-mortem tear down using pouch and cylindrical cells over a period of up to 3 months, to understand the characteristic consequences of embedding foreign elements into a cell. In summary, our approach provides information not yet available to researchers and cell manufacturers permitting improvements in performance and safety for existing technology as well as facilitating future innovation in cell design and management.

2. Experimental

In an attempt to demonstrate the universality of our approach, we have evaluated two distinct types of cells; pouch cells and automotive grade cylindrical cells, commonly used in Electric Vehicles [EVs] production. Commercial cylindrical cells show a high specific energy of around 3000 mAh within a volume of 16.54 cm^3 and are a highly standardised mechanical format. While pouch formations are more flexible in form factor, enabling varied applications, they require significant thermal and mechanical support from the battery module structure. These two types of cells are typically used in the Tesla EVs and Nissan Leaf respectively and therefore represent good case studies for this work.

2.1. Sensors fabrication

For temperature sensing raw NTC thermistor elements (Murata©) were selected due to a high precision, near linear beta curve, wide availability and a temperature range of -20 °C to 120 °C [26]. A 25 µm flexible Kapton© tape was used as a substrate for the thermistor elements - selected for its mechanical, chemical and thermal conductivity properties additionally, the material is readily available in a standard manufacturing setup. The raw thermistor elements were bonded onto the substrate using standard re-flow soldering technology.

In order to enable long-term in-situ measurements and extend the lifetime of the devices within the instrumented Li-ion cells, before embedding them (the thermistor elements and Kapton substrate) were protected by a conformal 1 µm coating of Parylene deposited using a PDS 2010 Labcoter® 2 (*Specialty Coating Systems*), offering significantly extended lifetime of the devices within harsh Li-ion cell environment. Parylene C, a polymer with excellent mechanical and chemical stability, is widely used for its barrier properties due to a pinhole free and highly conformal coating. Parylene C was evaluated in a range of harsh environments and even though delamination and limited protection were reported with structured layers, its barrier properties are excellent in case the integrity of the film is not compromised [27,28]. This was confirmed in this study by forming a uniform non-porous layer, protecting the sensor from electrical, chemical and mechanical interactions. Our results show that this approach enabled stable measurements and after over 3 months did not have an effect on the cells' or the thermistors' performances.

2.2. Instrumentation

Thermistors have several engineering design challenges that need to be addressed, including a non-linear response. Each thermistor node is arranged in series with a 0.1% precision resistor and a 0.1% voltage excitation source, effectively forming a voltage divider circuit. The voltage is measured between the two resistive elements - this configuration has the advantage of a minimum self-heating, an inherent resistance to voltage converter and signal linearisation. The voltage measurement is converted to temperature using the Steinhart-Hart equation (1) in software. A 14-bit data logging device (PicoLog) was used to interface with the sensor array.

$$T = \frac{B}{In\left(\frac{R_{Thermistor}}{R_0 \, x \, e^{\frac{-B}{T_0}}}\right)} \quad (1)$$

Where: B is the beta coefficient of thermistor element, R_0 is nominal resistance at room temperature, T_0 = temperature at R_0 and $R_{Thermistor}$ is the measured resistance of the element

Calibration of the sensors built this way is of high importance in order to avoid measurement errors which would otherwise lead to distorted data, false results and repeatability issues. Therefore, we have performed a thorough calibration using a thermal chamber and a high accuracy platinum resistance temperature detector (RTD) PT100 (*Pico®*) with a UKCAS accredit test certificate. The thermistor devices in question have an operating range of -20 °C to 120 °C and the manufacturer stated beta coefficients are evaluated over several discrete temperature spans. Each element on the substrate requires an individual calibration curve plotting over the operating span of the sensor. We have also confirmed that the Parylene coating did not affect the sensitivity, thermal response and characteristic curve of sensor elements by testing a batch of sensors via an accredited test house (*Taylor Instrument services*) for validation versus raw thermistor elements with no conformal coating - no response aberration was observed. Finally, we have performed another calibration post embedding within the cells.

2.3. Sensor to cell implementation

The pouch cells evaluated for the *in-situ* sensors application were 15-layer pouches built in house with a nominal capacity of 5.5 Ah, consisting of a lithium cobalt oxide ($LCoO_2$) cathode, graphite anode and a $LiPF_6$ electrolyte solution. Before the stack was sealed it was pried

open and the sensor slipped between the middle layers. A double layer of hot melt adhesive (polymer tape) was added to both sides of the sensor to form a complete seal. This procedure ensures no electrolyte leakage is possible, which was further confirmed by weighing of the instrumented cells before and after testing, as well as via cell cycling and impedance measurements.

The cylindrical cells evaluated for in-situ sensors applications were commercial 3 Ah high-energy cells consisting of a lithium nickel cobalt aluminium oxide (NCA) cathode, graphite anode and a $LiPF_6$ electrolyte solution. The cells were discharged to the minimum voltage of 2.5 V before being transferred into an argon glove box with atmospheric O_2 and H_2O concentrations of < 1 ppm. The cells were modified by removing the cathode cap and inserting the sensor directly into the mandrel core. The cap was the re-attached and sealed using a two-component epoxy to ensure gas tightness. Modifying the cell to the degree described here would not be necessary in an industrial application as a custom design could be implemented in the fabrication process.

2.4. Cell cycling

In order to mimic the behaviour of a typical cell during its operation, we have performed test cycles consisting of constant-current (CC) followed by constant-voltage (CV) charge and constant-current (CC) discharge, which is a standard for the lithium-ion chemistry. Furthermore, advanced pulsed or variable-current cycling techniques were explored in this study as they are key to developing rapid-(dis) charging profiles [29,16]. Finally, the stability of a long-term smart cells operation was evaluated through extended cycling. The pouch cells under investigation were placed under pressure during formation and cycling – consequently simulating real-life conditions of large scale battery systems. Approximately 2850 N/ m^2 were applied to each cell.

Evaluated cells were cycled between 2.5 V (0% SoC) and 4.2 V (100% SoC), utilising their full capacity range. The cycling rates for the CC/CV charge were 550 mA (C/10) for the 5.5 Ah pouch cells and 1 A (C/3) charge 3 A (1 C) discharge for the 3 Ah cylindrical 18,650 cells. For rapid discharge characterisation a 60 s period drawing 10 A (3.3C) was repeatedly applied until a minimum terminal voltage of 2.5 V was reached.

The cell characterisation cyclers used for this experimentation were VMP3 multi-channel potentiostats (*Bio-Logic Science Instruments*®). Calibration of all sensing equipment was conducted where possible near the time of the experiment. All experiments were conducted in an environmental chamber maintaining an ambient temperature of 25 °C (+/− 0.1 °C). Additionally, all testing equipment was warmed up for 4 h before experimentation to reduce the effects of analogue measurement error due to temperature variations. For interrogating the thermistor elements implemented within the cells a 14-bit analogue to digital converter PicoLog (*Pico*®) was used.

3. Results and discussion

We present our results in three parts. We first describe the data obtained via the sensing methodology applied. Then we discuss the stability of the smart cells. Finally, we evaluate the resistance of the sensor elements to the internal cell environment.

3.1. The in-situ distributed sensor provides new insights into cell performance and safety

In this section, we show how our data can be used to improve the performance of the cells. The data in Fig. 1 show the internal core and surface temperature during the charge/discharge phase of the cell. The temperature spikes observed during cell-cycling correlate tightly with the constant current/constant voltage phases. Even though no lag is observed between the core and the skin temperature, it is clear that in all cases presented the core temperature is significantly higher than the skin temperature.

The case of a rapid pulse discharge, which mimics what a cell can experience e.g. when an EV accelerates repeatedly, is represented in Fig. 1(A). The high temperature observed results from Joule heating due to the high internal resistances of high-energy Li-ion cells [30,31] and exothermic electrode material changes [7]. It is observed that the *in-situ* data temperature is showing a significant difference compared to the skin of the battery. In particular, it shows that the maximum core temperature reaches 81 °C, which is > 20 °C above the electrolyte stability limit. Additionally, a clear thermal gradient is also apparent within the cell core between the top and bottom zones, respectively the cathode (positive) and anode (negative) current collector connections. The gradient is possible due to the anisotropic heat conduction inside the cell and the current collector being the preferential heat transfer path. This subsequently results in local heat zones and heat induced mechanical stress from the temperature gradient [18,32]. The graph shows in fact that the safety limits of the cell operation is breached halfway throughout the discharge, significantly earlier than the external temperature sensor would suggest. When the safety temperature limits are breached, the reaction rates for the decomposition of the electrolyte and electrode materials increases, which can lead to the materials breakdown and gas formation, resulting in pressure build-up in the cell [8]. This creates a very high risk of the cell undergoing thermal runaway [7] and explosion or a sharp cycle life shortening [15,33]. Such internal damage is much more challenging to detect for a standard BMS and can lead to a catastrophic event if experienced repeatedly [7]. The ability to closely observe the cell's internal temperatures is paramount in solving these issues.

The second case presented show how our approach can drive the performance improvement of current cells. Fast charging of batteries is highly desirable however; it is often limited by safety concerns. Through the real-time measurement of the internal (core) temperature, we demonstrate that cells can be charged significantly faster than the manufacturer's recommendation without exceeding the thermal safety limits. Fig. 1B shows that, even though the cell is being charged at 2.2 C rather than following the manufacturers rating of C/3, the internal temperature remains below the recommended safety limits, dictated by the stability of the electrolyte [7,16]. This clearly shows that, under the manufacturer's guidelines, these cells are not currently operating near their maximum performance. Therefore, our method of monitoring of internal operando temperatures can open up opportunities for innovation in cells performance. The results obtained in this study confirm our previous work, where, using optical sensor monitoring, we have demonstrated that a 0-to-80% charge can be achieved in only 30 min through the implementation of a rapid-charging profile instead of 2 h and 40 min (as per manufacturer guideline), a five-fold reduction in charging time [16]. Therefore, the approach proposed in this work, using a distributed array of thermistors that addresses the issues typically encountered when using optical sensor [16,18], such as cross-sensitivity and low flexibility, represents a viable solution for battery management as they can be designed for any cell format, ensuring no hot-spots omission.

Lastly, Fig. 2 shows a full distributed view of a sensing array data collected from the core of a cylindrical 18,650 cell. The data clearly portrays a near uniformity of temperature within the core, but a significant differential between the core and skin temperature is apparent and expected. The core temperature uniformity is possible due to the mandrel (cell component used in manufacturing of cells), enabling as a low resistance thermal path and thus uniformity within the core is present. However, this observation will vary between different cell constructions as previous studies [18] using distributed core measurements identified a clear temperature differential within the core. Furthermore, the temperature sensors responded with no visible lag and have a temperature sensitivity of 0.1 °C, concluding that the readings obtained are highly accurate and stable.

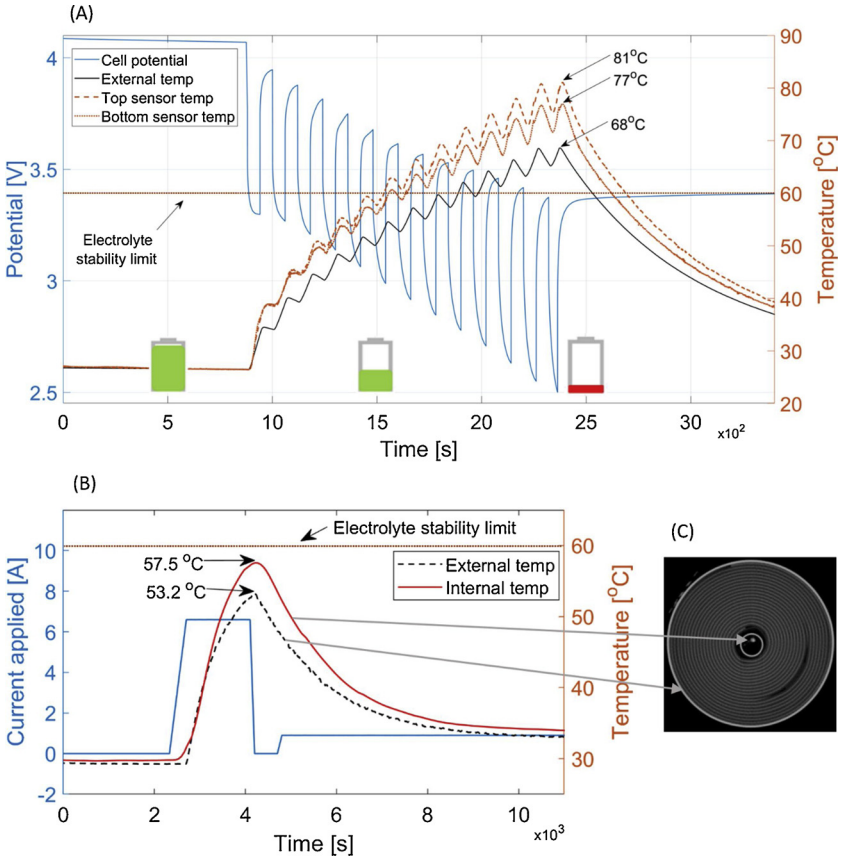

Fig. 1. Lithium-ion cell *in-situ* and skin temperature changes under a high current load. Heavy pulse discharge (A) is mimicking irregular electric vehicle acceleration until the batteries are fully drained, while a high charge current (B) is relevant to rapid charging profiles development. Panel (C) shows a top-view X-ray image of an instrumented cell. Clear and increasing difference between the internal and external cell temperatures can be observed.

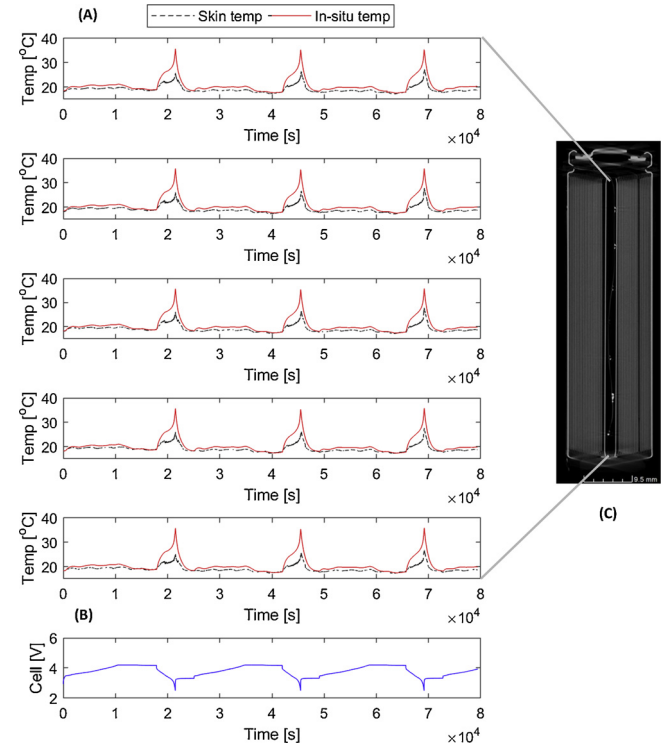

Fig. 2. Distributed sensor array in cylindrical cells. In this case, 5 sensors are distributed along the length of the cell, thus ensuring no hot-spot omissions. (A), and the corresponding cell potential (B), collected from an 18650 cell (C).

3.2. Stability of the smart cell systems

Here we evaluate the stability of the sensor for long-term, operando measurement in the harsh environment of the cells. We also show that the integration of the distributed sensor does not affect the performance of the cells. In particular, we evaluate the sensors readings stability and the cell capacity retention, a commonly agreed indicator of the Li-ion cells' SoH. Typically, cells are considered at their end-of-life when the capacity falls below 80% of the rated value [34].

3.2.1. Stability of the sensors

It is important that the sensors do not suffer any negative impact due to their operation within the corrosive environment of the cells. Exposure to the organic solvents and HF present in the electrolyte leads to rapid corrosion of any uncoated tracks and sensing elements. The stability of the distributed sensor was evaluated by comparing the readings of pristine, uncoated sensor and sensors coated with a 1 µm thick Parylene C layer. Fig. 3(A) shows the temperature data of a coated and uncoated sensors, positioned in a cylindrical cell in the same location. A 10 h measurement is sufficient to show major discrepancies between uncoated sensor (broken line) and the coated sensor (solid line). The erratic behaviour of the uncoated sensors, noted after 100 min only, is due to the corrosion of the sensor as confirmed by the broken sensor analysis - shown in the supplementary materials. The coated sensors were also evaluated for long-term stability and were successfully embedded in cells for 3 months under normal conditions, suggesting that such sensors can be used during the lifetime of cells in regular deployment. Cycled sensors are also analysed post-mortem in a later section, where no visible degradation is noted.

3.2.2. Time domain analysis – cyclic aging

Next, it is important to show that the integration of the sensor does not have any negative impact on the cell stability. To do so, we have

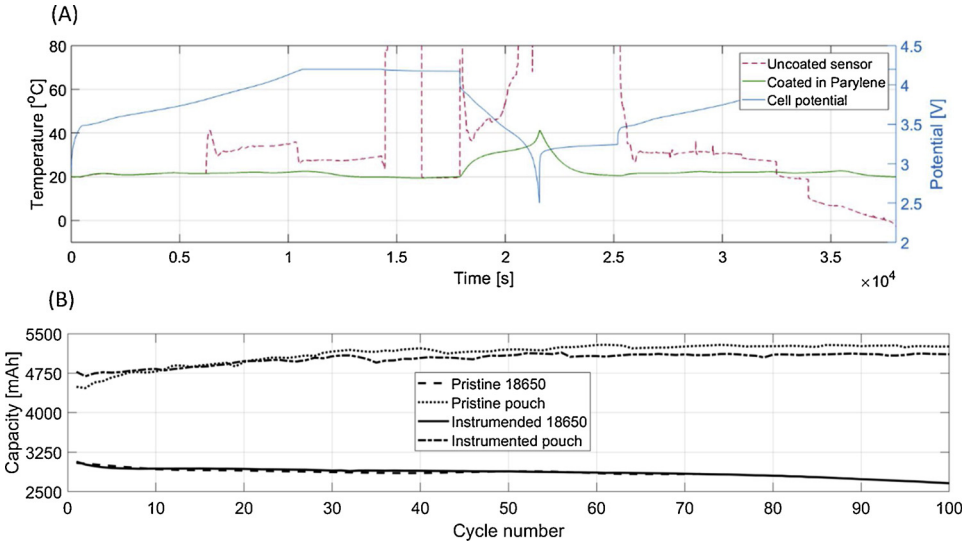

Fig. 3. Instrumented cells - sensors comparison (A) and cycling capacity data (B). Cells were cycled using their standard cycling profiles between 2.5 V and 4.2 V. Panel (A) shows how uncoated sensors (broken red line) fail almost instantly in the harsh cell environment, while the applied Parylene coating (solid green line) resolves this issue, ensuring sensor longevity. Panel (B) indicates that good capacity retention is present, on par with the non-modified cells, proving the negligible modification impact point over 100 full cycles (For interpretation of the references to colour in this figure legend, the reader is referred to the web version of this article).

performed cyclic aging on the cells according to the manufacturer guidelines at a rate of 565 mA (C/10) for pouch and at 1 A (C/3) charge and 3 A (1C) discharge for the cylindrical 18,650 s. The systems under investigation show no significant differences between modified and unmodified cells capacity, as shown in Fig. 3(B). The data shown represents capacity values extracted from 100 cycle data set – cycling profiles are available in the supplementary material. The data presented clearly shows that the cells have not suffered any electrolyte loss or cell material damage that could have been incurred during cell manufacturing and sensors insertion.

3.2.3. Frequency domain analysis - Impedance behaviour

Another important parameter indicative of the cells' internal health is the electrochemical impedance response. The instrumented cells were analysed and compared against pristine cells using Electrochemical Impedance Spectroscopy [35] (EIS), a highly sensitive dielectric spectroscopy method used to observe the impedance response of a system over a range of alternating current (AC) signal frequencies, allowing for energy storage and dissipation properties comparison. The method is capable of detecting issues such as minor electrolyte loss or a localized electrode damage that would not have been detected in the time domain analysis conducted in the previous section. Fig. 4 represents the evaluated cells characteristic impedance responses via Nyquist plots and shows that the applied modifications have a negligible effect on the overall system performance.

The EIS profile of pouch cells in Fig. 4(A–B) shows no significant difference between normal and smart cells, although some shift in mid-frequency region can be observed, indicative of the charge transfer resistance increase. This shift can be explained with the surface impedance increase due to the sensor covering some of the active electrode area within the cell. This effect can be minimised by further optimising the sensors layout and substrate footprint reduction. The above corroborates the results obtained for cell cycling data (see Fig. 3B) confirming the negligible effect of the sensors insertion and operation on the overall cells performances.

In case of cylindrical cells' impedance behaviour in Fig. 4(C–D), minor changes can be noticed in the mid- and low-frequency region, which corresponds to the charge transfer and lithium diffusion phenomena respectively. These changes are a result of to the pressure relief caused by opening of the cells. Cylindrical cells are not normally degassed after formation [36], which results in increased internal pressure. Opening the cell releases this over-pressure and subsequently unblocks pores in the electrode active material enabling easier access to their surface. While of positive effect - reducing the diffusion and charge transfer resistances - such changes have negligible impact on the cell as shown in Fig. 3(B) and our previous work [16]. This phenomena can be avoided altogether in a manufacturing environment by embedding the sensing device during cell assembly instead of post-production. Consequently, no such effect is observable in case of pouch cells EIS responses, as the sensors were inserted during the cell production.

3.3. Smart cell construction, sensors and electrodes inspection

As the thermal responses of the cells are most often non-uniform [37], precise placement of the sensing element is imperative for accurate monitoring of their behaviour. We have used X-ray Computed Tomography (X-TEK XTH 320 LC, *Metris*) to identify the most appropriate sensor location within the cells and to evaluate the effect of the sensors integration on the cells.

In case of the soft pouch cell, the thermistor elements were located at the center of the electrode stack, where significant thermal difference is expected compared to the surface. The horizontal lines observed are shadowing effects caused by higher X-ray beam attenuation of the thermistor elements and are not actual physical defects.

For cylindrical cells, the location was chosen to coincide with the core, where access is readily available and, most importantly, hot-spot formation is highly likely due to the centralized cylindrical cell geometry. Besides, in this location the sensor is less likely to damage electrode material or interfere with internal battery processes. Fig. 5H shows *in-situ* X-Ray images of the sensors inserted within a cylindrical cell. It is noted that the cathode cap adjustment and the indirect sensor insertion path would not be required in a manufacturing environment as a custom made cap could be pre-made with a sensor entry point.

In order to evaluate the integrity of the sealing methods and any potential loss of electrolyte solution, the cells were weighed using a laboratory scale accurate to 1 mg. Before and after cycling for pouch cells and before and after modification for cylindrical cells. No differences in mass were observed, which – together with stable impedance and cycling results - proves that the sealing method of hot-melt polymer tape for pouch cells is an effective solution, and did not result in electrolyte loss at insertion or during the cell operation.

For cylindrical cells, as the electrolyte is completely soaked into the separator and active materials acting as a sponge, no loss is expected during the modification. The mass before and after modification was measured to be 45.8 g and 46 g respectively, which then remained stable confirming successful sealing of the cell. The increased weight is in agreement with the added mass from modification. Furthermore, as shown by the time and frequency domain analysis conducted in this

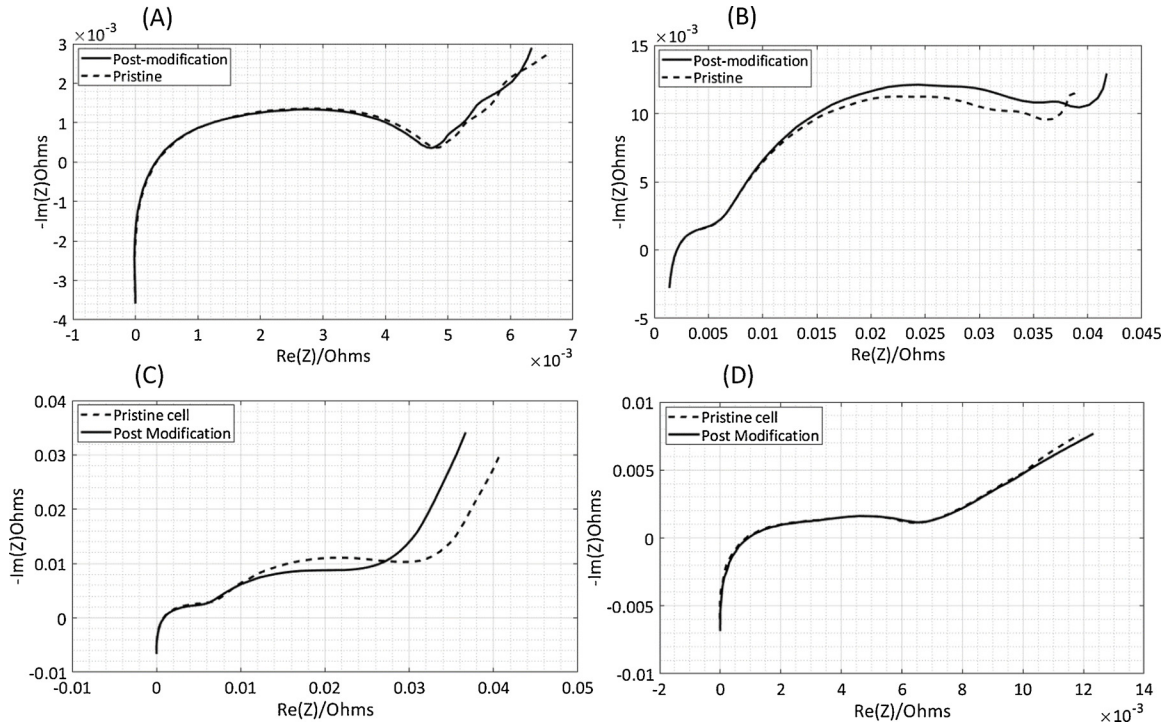

Fig. 4. EIS study of the cylindrical and pouch cells pre- and post-modification. It is visible that sensors insertion causes negligible changes to the cells' EIS responses. Pouch cell responses are shown in panel A and B, 100% and 0% SoC respectively, while cylindrical cell behaviour is represented in panel C (100% SoC) and D (0% SoC).

study, the modification procedure had no noticeable effect upon the cell performance.

We then evaluated the influence of the long-term operation of the coated sensors within the harsh cells environment by observing used sensors under a microscope. Fig. 6(A–E) show coated sensors removed from the cells after 1 month of cycling under normal conditions. It is apparent that the thermistor elements and copper tracks are intact. Fig. 6(F) shows a detail of the negative electrode material that was in close proximity to the sensor. Our concern in this area was a potential for lithium plating and capacity loss because the electrode area covered by the sensor could have increased surface impedance and limited access. The sensor inherent mechanical design indicates that a slight bump can be present where the thermistor elements are located. It is important to evaluate this parameters, because such bumps, if geometrically significant, can lead to electrolyte welling and subsequent lithium plating, or in extreme cases mechanical damage. This can be especially pronounces when under pressure that cells experience when assembled into a real-life large scale battery system. However, it was found to be of negligible effect on the cells performance, despite the added pressure, as shown in the previous impedance and cycling ageing undertaken in this study. The result are overall very promising for the sensing methodology shown here, which, with further reduction of the sensing array surface area and mechanical height of the elements, can be seamlessly integrated into the manufacturing process, leading to a range of smart cell devices.

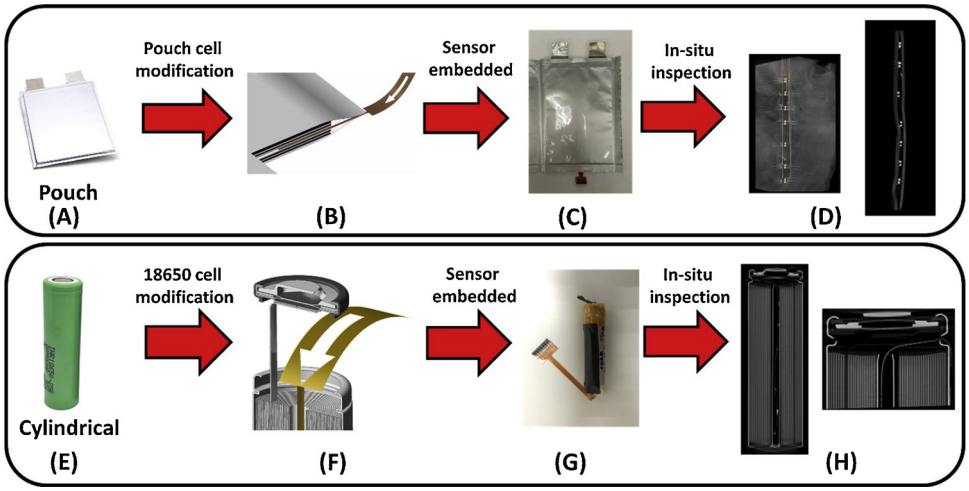

Fig. 5. Smart cells construction. (A) and (E) show unmodified cells, (B) and (F) represent sensor inserted during manufacturing, (C) and (G) are images of complete instrumented cells and (D) and (H) show in-situ X-ray images of the cells post-modification.

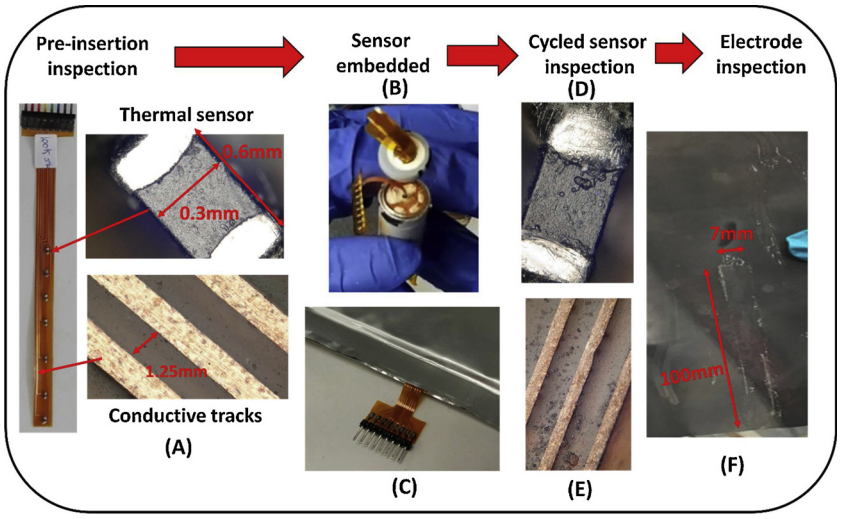

Fig. 6. Analysis of the sensors pre- and post-cycling. Panel (A) represents pristine sensor before embedding into a cell. (B) and (C) show cells inspected after cycling. (D) and (E) demonstrate sensor elements retrieved from the cell – some electrolyte residue can be seen in these images. (F) is a cycled electrode material from an instrumented pouch cell.

4. Conclusions

The objective of this study was to develop and evaluate a novel *in-situ* sensing methodology for Li-ion energy storage. We propose a widely applicable smart cell concept enabling unprecedented high-precision *in-situ* and operando thermal monitoring of pouch and cylindrical format batteries. High-fidelity thermal responses from inside the cell were successfully monitored under various cycling conditions, most notably demonstrating a significant divergence between the core and skin cell temperatures, impacting the perceived cell safety. Importantly, our smart cells successfully detected rapid temperature changes with no response lag. Moreover, we have demonstrated that the cell charging time can be significantly reduced without compromising the thermal safety limit. We have also shown that under particular scenarios safety limits can be breached earlier than the external sensors would indicate, leading to a false sense of security or faster degradation. The sensor topology, polymer encapsulation and the cell modifications to adapt the sensing methodology were proven to be durable, enabling long term in operando monitoring while having no adverse effect on the cells performance.

To thoroughly evaluate the smart cells design, we used several in-depth characterisation methods - X-ray imaging was used to confirm the central location of the sensors, essential for hot-spots detection; electrochemical impedance spectroscopy and repetitive cycling over a sustained period of time was deployed to assess the cell's electrochemical performance as on-par with unmodified commercial cells. Finally, a full cell tear-down and sensor inspection followed confirming the sensors resistance to the cell's harsh internal environment, key to long-term operation of the smart cells.

This work shows that our proposed *in-situ* sensing approach has the potential to drive improvement in both performance and operational safety mapping. The thermal data gathered with the use of the smart cells represents a vital source of key information, critical for the battery management systems to maintain a most optimal performance and an up-to-date understanding of the cells State of Health during deployment in real-life scenarios. Finally, it is foreseen that the sensing methodology developed here will support the design, research and rapid prototyping of new cells and smart battery modules, enabling considerably greater performance to be safely harnessed from these increasingly prevalent Li-ion energy storage systems.

Data statement

The datasets generated during and analysed during the current study are available from the corresponding author on a reasonable request.

Some restrictions apply to the availability of the data on the commercial cells used for this study.

Author Information & Acknowledgments

The authors declare no competing financial interests. Correspondence and requests for materials should be addresses to: t.amietszajew.1@warwick.ac.uk.

J.F, T.A., A.J.R. and J.C. performed the experiments and analysed the data. R.B. and D.G. supervised the project and offered advice. All authors designed the experiments and wrote the manuscript. Thanks to M. Maharun for support with figures design.

This research received funding from Jaguar Land Rover and EPSRC. This research was done with support from the TRENDS project (reference number EP/R020973/1).

Appendix A. Supplementary data

Supplementary material related to this article can be found, in the online version, at doi:https://doi.org/10.1016/j.est.2019.01.026.

References

[1] F.J. Dyson, Search for artificial stellar sources of infrared radiation, Science (80-) 131 (1960) 1667–1668, https://doi.org/10.1126/science.131.3414.1667.
[2] C.J. Bae, A. Manandhar, P. Kiesel, A. Raghavan, Monitoring the strain evolution of lithium-ion battery electrodes using an optical Fiber bragg grating sensor, Energy Technol. 831 (2016), https://doi.org/10.1002/ente.201500514.
[3] A. Opitz, P. Badami, L. Shen, K. Vignarooban, A.M. Kannan, Can Li-Ion batteries be the panacea for automotive applications? Renew. Sustain. Energy Rev. 68 (2017) 685–692, https://doi.org/10.1016/j.rser.2016.10.019.
[4] B. Nykvist, M. Nilsson, Rapidly falling costs of battery packs for electric vehicles, Nat. Clim. Chang. 5 (2015) 329–332, https://doi.org/10.1038/nclimate2564.
[5] P. Miller, Automotive lithium-ion batteries, Johnson Matthey Technol. Rev. 59 (2015) 4–13, https://doi.org/10.1595/205651315X685445.
[6] B. Scrosati, J. Garche, Lithium batteries: status, prospects and future, J. Power Sources 195 (2010) 2419–2430, https://doi.org/10.1016/j.jpowsour.2009.11.048.
[7] Q. Wang, P. Ping, X. Zhao, G. Chu, J. Sun, C. Chen, Thermal runaway caused fire and explosion of lithium ion battery, J. Power Sources 208 (2012) 210–224, https://doi.org/10.1016/j.jpowsour.2012.02.038.
[8] I. Bloom, S.A. Jones, E.G. Polzin, V.S. Battaglia, G.L. Henriksen, C.G. Motloch, R.B. Wright, R.G. Jungst, H.L. Case, D.H. Doughty, Mechanisms of impedance rise in high-power, lithium-ion cells, J. Power Sources 111 (2002) 152–159.
[9] D. Deng, Li-ion batteries: basics, progress, and challenges, Energy Sci. Eng. 3 (2015) 385–418, https://doi.org/10.1002/ese3.95.
[10] N. Martiny, A. Rheinfeld, J. Geder, Y. Wang, W. Kraus, A. Jossen, Development of a thin-film thermocouple matrix for in-situ temperature measurement in a lithium ion pouch cell, IEEE Sens. J. (2014) 3377–3384, https://doi.org/10.1109/JSEN.2014.2331996 (1)TUM CREATE (2)Institute for Technical Electronics, Technical University of Munich (3)Institute for Electrical Energy Storage Technology, Technical University of Munich.

[11] L.H. Saw, Y. Ye, A.A.O. Tay, W.T. Chong, S.H. Kuan, M.C. Yew, Computational fluid dynamic and thermal analysis of Lithium-ion battery pack with air cooling, Appl. Energy 177 (2016) 783–792, https://doi.org/10.1016/j.apenergy.2016.05.122.
[12] BBC, Authorities Investigate After Tesla Car Catches Fire, Website, (2016) https://www.bbc.co.uk/news/technology-37104753.
[13] P. Bohn, G. Liebig, L. Komsiyska, G. Wittstock, Temperature propagation in prismatic lithium-ion-cells after short term thermal stress, J. Power Sources 313 (2016) 30–36, https://doi.org/10.1016/j.jpowsour.2016.02.055.
[14] T. Waldmann, G. Bisle, B.I. Hogg, S. Stumpp, M.A. Danzer, M. Kasper, P. Axmann, M. Wohlfahrt-Mehrens, Influence of cell design on temperatures and temperature gradients in lithium-ion cells: an in operando study, J. Electrochem. Soc. 162 (2015) A921–A927, https://doi.org/10.1149/2.0561506jes.
[15] E. McTurk, T. Amietszajew, J. Fleming, R. Bhagat, Thermo-electrochemical instrumentation of cylindrical Li-ion cells, J. Power Sources 379 (2018) 309–316, https://doi.org/10.1016/j.jpowsour.2018.01.060.
[16] T. Amietszajew, E. McTurk, J. Fleming, R. Bhagat, Understanding the limits of rapid charging using instrumented commercial 18650 high-energy Li-ion cells, Electrochim. Acta 263 (2018) 346–352, https://doi.org/10.1016/j.electacta.2018.01.076.
[17] S. Panchal, I. Dincer, M. Agelin-Chaab, R. Fraser, M. Fowler, Thermal modeling and validation of temperature distributions in a prismatic lithium-ion battery at different discharge rates and varying boundary conditions, Appl. Therm. Eng. 96 (2016) 190–199, https://doi.org/10.1016/j.applthermaleng.2015.11.019.
[18] J. Fleming, T. Amietszajew, E. McTurk, D. Greenwood, R. Bhagat, G. Dave, R. Bhagat, E. McTurk, D. Greenwood, R. Bhagat, Development and evaluation of in-situ instrumentation for cylindrical Li-ion cells using fibre optic sensors, HardwareX. 3 (2018) 100–109, https://doi.org/10.1016/j.ohx.2018.04.001.
[19] N.S. Spinner, K.M. Hinnant, R. Mazurick, A. Brandon, S.L. Rose-pehrsson, S.G. Tuttle, Novel 18650 lithium-ion battery surrogate cell design with anisotropic thermophysical properties for studying failure events, J. Power Sources 312 (2016) 1–11, https://doi.org/10.1016/j.jpowsour.2016.01.107.
[20] P.J. Osswald, S.V. Erhard, J. Wilhelm, H.E. Hoster, A. Jossen, Simulation and measurement of local potentials of modified commercial cylindrical cells: I. Cell preparation and measurements, J. Electrochem. Soc. 162 (2015) A2099–A2105, https://doi.org/10.1149/2.0561510jes.
[21] T. Waldmann, M. Wohlfahrt-Mehrens, In-operando measurement of temperature gradients in cylindrical lithium-ion cells during high-current discharge, ECS electrochem, Lett. 4 (2015) A1–A3, https://doi.org/10.1149/2.0031501eel.
[22] G. Zhang, L. Cao, S. Ge, C.Y. Wang, C.E. Shaffer, C.D. Rahn, In situ measurement of radial temperature distributions in cylindrical Li-Ion cells, J. Electrochem. Soc. 161 (2014) A1499–A1507, https://doi.org/10.1149/2.0051410jes.
[23] C. Forgez, D. Vinh Do, G. Friedrich, M. Morcrette, C. Delacourt, Thermal modeling of a cylindrical LiFePO4/graphite lithium-ion battery, J. Power Sources 195 (2010) 2961–2968, https://doi.org/10.1016/j.jpowsour.2009.10.105.
[24] N. Martiny, A. Rheinfeld, J. Geder, Y. Wang, W. Kraus, A. Jossen, Development of an all kapton-based thin-film thermocouple matrix for in situ temperature measurement in a lithium ion pouch cell, IEEE Sens. J. 14 (2014) 3377–3384, https://doi.org/10.1109/JSEN.2014.2331996.
[25] M.S.K. Mutyala, J. Zhao, J. Li, H. Pan, C. Yuan, X. Li, In-situ temperature measurement in lithium ion battery by transferable flexible thin film thermocouples, J. Power Sources 260 (2014) 43–49, https://doi.org/10.1016/j.jpowsour.2014.03.004.
[26] NCP03WF104F05RL Specifications, (2018), pp. 4–6 https://www.murata.com/en-sg/api/pdfdownloadapi?cate=luNTCforTempeSenso&partno=NCP03WF104F05RL.
[27] W. Li, D.C. Rodger, E. Meng, J.D. Weiland, M.S. Humayun, Y.C. Tai, Flexible parylene packaged intraocular coil for retinal prostheses, Proc. 2006 Int. Conf. Microtechnologies Med. Biol. (2006) 105–108, https://doi.org/10.1109/MMB.2006.251502.
[28] J. Charmet, J. Bitterli, O. Sereda, M. Liley, P. Renaud, H. Keppner, Optimizing parylene C adhesion for MEMS processes: potassium hydroxide wet etching, J. Microelectromech. Syst. 22 (2013) 855–864, https://doi.org/10.1109/JMEMS.2013.2248126.
[29] P. Keil, A. Jossen, Charging protocols for lithium-ion batteries and their impact on cycle life-An experimental study with different 18650 high-power cells, J. Energy Storage. 6 (2016) 125–141, https://doi.org/10.1016/j.est.2016.02.005.
[30] P.V. Braun, J. Cho, J.H. Pikul, W.P. King, H. Zhang, High power rechargeable batteries, Curr. Opin. Solid State Mater. Sci. 16 (2012) 186–198, https://doi.org/10.1016/j.cossms.2012.05.002.
[31] K.E. Aifantis, S.A. Hackney, V. Kumar, High Energy Density Lithium Batteries: Materials, Engineering, Applications, Wiley-VCH Verlag GmbH & Co., KGaA, 2010, https://doi.org/10.1002/9783527630011.
[32] Y. Zhao, Y. Patel, T. Zhang, G.J. Offer, Modeling the effects of thermal gradients induced by Tab and surface cooling on Lithium ion cell performance, J. Electrochem. Soc. 165 (2018) A3169–A3178, https://doi.org/10.1149/2.0901813jes.
[33] L. Jiling, Z. Zhen, battery Thermal Management Systems of Electric Vehicles, Chalmers University of Technology, 2014.
[34] M. Dubarry, B.Y. Liaw, Identify capacity fading mechanism in a commercial LiFePO4 cell, J. Power Sources 194 (2009) 541–549, https://doi.org/10.1016/j.jpowsour.2009.05.036.
[35] S.M.M. Alavi, C.R. Birkl, D.A. Howey, Time-domain fitting of battery electrochemical impedance models, J. Power Sources 288 (2015) 345–352, https://doi.org/10.1016/j.jpowsour.2015.04.099.
[36] Y. Masaki, R.J. Brodd, A. Kozawa, Lithium-Ion Batteries, Springer, New York, 2009, https://doi.org/10.1007/978-0-387-34445-4_8.
[37] S. Goutam, J.M. Timmermans, N. Omar, P. Van den Bossche, J. Van Mierlo, Comparative study of surface temperature behavior of commercial li-ion pouch cells of different chemistries and capacities by infrared thermography, Energies 8 (2015) 8175–8192, https://doi.org/10.3390/en8088175.